Structural Model of the BCL-w−BID Peptide Complex and Its Interactions with Phospholipid Micelles[†,‡]

Alexey Yu. Denisov,[§] Gang Chen,[||,⊥] Tara Sprules,[@] Tudor Moldoveanu,[§] Pierre Beauparlant,[||] and Kalle Gehring*[,§,@]

Department of Biochemistry and Quebec/Eastern Canada High Field NMR Centre, McGill University, Montreal, Quebec H3G 1Y6, Canada, and Gemin X Biotechnologies Inc., Place du Parc, Montreal, Quebec H2X 4A5, Canada

Received November 15, 2005; Revised Manuscript Received December 20, 2005

ABSTRACT: A peptide corresponding to the BH3 region of the proapoptotic protein, BID, could be bound in the cleft of the antiapoptotic protein, BCL-w. This binding induced major conformational rearrangements in both the peptide and protein components of the complex and led to the displacement and unfolding of the BCL-w C-terminal α-helix. The structure of BCL-w with a bound BID-BH3 peptide was determined using NMR spectroscopy and molecular docking. These studies confirmed that a region of 16 residues of the BID-BH3 peptide is responsible for its strong binding to BCL-w and BCL-x_L. The interactions of BCL-w and the BID-BH3 peptide complex with dodecylphosphocholine micelles were characterized and showed that the conformational change of BCL-w upon lipid binding occurred at the same time as the release and unfolding of the BH3 peptide.

Programmed cell death (apoptosis) plays a key role in the removal of infected, damaged, or unwanted cells. The BCL-2 family of proteins is a crucial regulator of this process (*1*−*4*). Members of the BCL-2 family possess up to four conserved BCL-2 homology (BH) regions and can be divided into three groups: antiapoptotic proteins (BCL-2, BCL-x_L, BCL-w, MCL-1, and A1), proapoptotic multi-BH region proteins (BAX, BAK, and BOK), and proapoptotic BH3-only proteins (BID, BAD, BIM, BIK, BMF, PUMA, NOXA, and HRK). Imbalance in the levels of BCL-2 family proteins can result in cancer, autoimmunity, Alzheimer's disease, and other serious diseases. Once the prosurvival proteins are neutralized by BH3 ligands (*5*), proapoptotic members BAX and BAK can be activated by cleaved BID, detergents, or heat to oligomerize and form supramolecular openings in the outer mitochondrial membrane, which leads to cytochrome *c* release and mitochondrial-dependent apoptosis (*6*, *7*). It was also shown that the upstream death stimulus p53 could activate BAX and BAK in the absence of other proteins and causes disruption of complexes for both the proapoptotic multi-BH region or the BH3-only protein with antiapoptotic proteins (*8*, *9*).

The structural biology of the BCL-2 family of proteins has developed significantly during the past decade (*10*), as structures of prosurvival BCL-x_L (*11*, *12*), BCL-w (*13*, *14*), BCL-2 (*15*, *16*), MCL-1 (*17*), proapoptotic BID (*18*, *19*), BAX (*20*), and complexes of BCL-x_L with BAK, BAD, and BIM peptides (*21*−*23*) have been determined. However, structural studies of interactions of BCL-2 family proteins with lipid or lipidlike membranes are most challenging technically, and the main details have still not been resolved.

Possible approaches to studying membrane proteins by NMR[1] involve the use of detergent micelles in solution as a mimic of membranelike environments or solid-state NMR methods applied to membrane proteins in planar lipid bilayers. NMR studies of BCL-x_L (*24*, *25*) and truncated tBID (*26*) proteins demonstrate different aspects of their binding to membranes. The two central hydrophobic helices, α5 and α6, of BCL-x_L supposedly insert into membranes to participate in channel forming, like colicins or the transmembrane domain of diphtheria toxin (*27*), while the helices of apoptotic activator tBID are mostly parallel to the membrane surface. The NMR results for binding of tBID to the membrane were confirmed by site-directed spin labeling methods for EPR spectroscopy (*28*). In general, these analyses are complicated, because the membrane conformation of BCL proteins can be changed during the induction of apoptosis as was shown for BCL-2 (*29*). Also, tBID could interact with BAX not only via protein−protein BH3-dependent mechanisms but

[†] This work was supported by a strategic project grant from the Natural Sciences and Engineering Research Council (NSERC) of Canada. T.M. was supported by a fellowship from the Canadian Institutes of Health Research. K.G. is a Chercheur National of the Fonds de la recherche en santé de Québec.

[‡] The coordinates have been deposited as Protein Data Bank entry 1ZY3.

* To whom correspondence should be addressed: Department of Biochemistry, McGill University, 3655 Promenade Sir William Osler, Montreal, Quebec H3G 1Y6, Canada. Telephone: (514) 398-7287. Fax: (514) 847-0220. E-mail: kalle.gehring@mcgill.ca.

[§] Department of Biochemistry, McGill University.

[||] Gemin X Biotechnologies Inc.

[⊥] Current address: Institute de Recherches Cliniques de Montreal (IRCM), Montreal, Quebec H2W 1R7, Canada.

[@] Quebec/Eastern Canada High Field NMR Centre, McGill University.

[1] Abbreviations: DPC, dodecylphosphocholine; DTT, dithiothreitol; EDTA, ethylenediaminetetraacetic acid; EPR, electron paramagnetic resonance; GST, glutathione thiol transferase; HPLC, high-pressure chromatography; HSQC, heteronuclear single-quantum correlation; NMR, nuclear magnetic resonance; NOESY, nuclear Overhauser effect spectroscopy; rmsd, root-mean-square deviation.

10.1021/bi052332s CCC: $33.50
Published on Web 01/21/2006

also via protein−lipid interactions causing disruption of the lipid bilayer structure during apoptosis (*30*).

The prosurvival BCL-w protein is upregulated in colorectal cancer and plays an essential role in spermatogenesis (*31*−*33*). BCL-w is functionally similar to BCL-x_L and BCL-2, but BCL-w is located exclusively on the mitochondria (*34*). BCL-w is weakly attached to the mitochondrial membrane in healthy cells, and a tight membrane association is triggered only in dying cells upon binding of BH3-only proteins (*14*, *34*). The solution structure of BCL-w (*13*, *14*) reveals that the BCL-w C-terminal tail is not normally exposed but folds as an α-helix in the BH3-binding hydrophobic cleft of BCL-w, restricting random interactions with potential partners. The binding of the BH3 ligands releases the C-terminal region from the BCL-w cleft, thereby allowing its insertion into the membrane and neutralizing its survival function. Here, we continue our studies of the BCL-w protein (*13*) and report a model structure of BCL-w with a BH3 peptide. We also confirmed the previous finding of binding of detergent to individual BCL proteins (*20*, *24*). A working model for the interaction between the complex of the BCL-w protein with the BH3 peptide and membranes is presented for the first time.

EXPERIMENTAL PROCEDURES

Sample Preparation. Human BCL-w and mouse BCL-x_L, both lacking the C-terminal transmembrane regions but containing a C-terminal His tag, were prepared as described previously (*13*). The unlabeled 20-amino acid BH3 peptide of human BID (IIKNIARHLAQVGDSMDRSI) was chemically synthesized (BRI-NRC, Montreal, PQ). Other 30-amino acid peptides from the BH3 regions (residues 77−106) of human BID (ESQEDIIRNIARHLAQVGDSMDRSIP-PGLV) and mouse BID (ESQEEIIHNIARHLAQIGDEM-DHNIQPTLV) were subcloned into the pGEX-6P-1 vector and expressed as GST fusions in the *Escherichia coli* BL21-(Gold) strain. PreScission protease (Amersham Biosciences) was used for the cleavage of the fusion BH3 peptide from GST, which results in an extra GPLGS sequence at the N-termini of the peptide as a part of the cleavage site. For NMR, cultures were grown in M9 medium supplemented with [^{15}N]ammonium chloride and/or ^{13}C-enriched glucose to produce uniformly ^{15}N-labeled or ^{15}N- and ^{13}C-labeled proteins or peptides. Unexpectedly, the 30-amino acid BID-BH3 peptides were cleaved in the middle of BH3 region (between Ala-11 and Arg-12, according to mass spectral analysis following reverse phase HPLC) by an unknown protease during the initial steps of peptide purification. To avoid this major problem, we protected the BH3 peptide with the BCL-w protein as follows. *E. coli* BL21 cells expressing BCL-w were added to the BH3 peptide-expressing cells before the sonication, and BCL-w was removed later during the peptide purification by reverse phase HPLC. NMR samples contained BCL-w or 1:1 BCL protein−BH3 peptide complexes in a 90% H_2O/10% D_2O mixture, 20 mM sodium phosphate (pH 6.8−7.2), 0.5 mM EDTA, and 3 mM DTT. Protein and BH3 peptide concentrations were in the range of 0.05−0.1 mM for NMR titration experiments or 0.5−0.7 mM for three-dimensional NMR experiments for signal assignments. The detergents used in the studies were dodecylphosphocholine-d_{38} (DPC) from Cambridge Isotope Laboratories and *n*-octyl β-D-glucoside from Sigma.

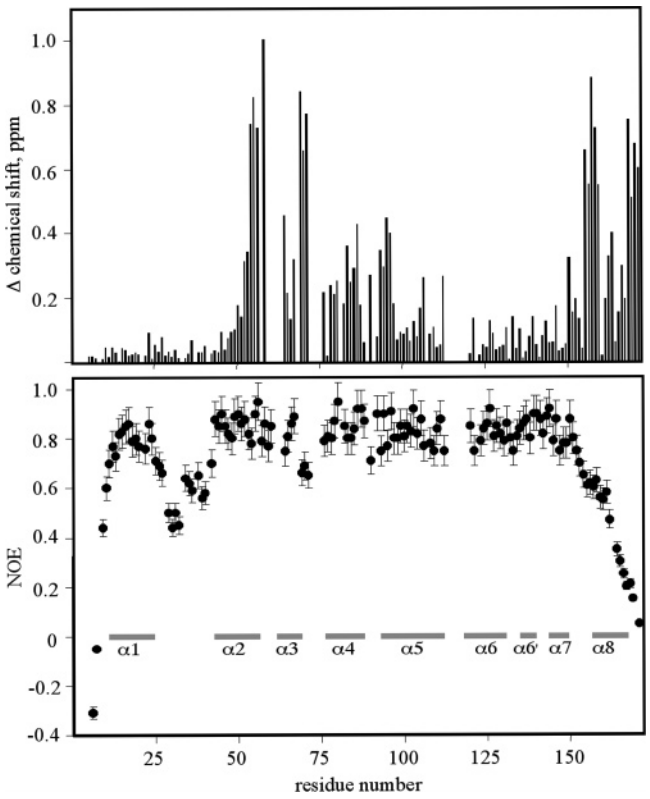

FIGURE 1: Identification of the BCL-w binding site for the BID-BH3 peptide. The top panel shows the magnitude of the amide chemical shift changes $\{[(\Delta^1\text{H shift})^2 + (\Delta^{15}\text{N shift} \times 0.2)^2]^{1/2}\}$ of BCL-w upon binding of the 20-amino acid human BID-BH3 peptide. The bottom panel shows values of the heteronuclear ^{15}N-{^{1}H} NOEs for backbone amides of BCL-w in complex with the BID-BH3 peptide. The positions of the eight α-helices in the solution structure of BCL-w are shown.

NMR Spectroscopy. NMR spectra were acquired at 25−30 °C on Bruker DRX 600 MHz and Varian Unity Inova 800 MHz spectrometers equipped with triple-resonance cryoprobes and pulsed field gradients. The following experiments were used for backbone and side chain ^{1}H, ^{13}C, and ^{15}N resonance assignments: HNCACB, CBCA(CO)HN, HNCA, and ^{15}N-edited TOCSY (*35*). Proton homonuclear NOEs were obtained from ^{15}N-edited NOESY spectra recorded at 800 MHz with a mixing time of 90 ms. ^{15}N-edited NOESY spectra with and without ^{13}C decoupling (refocusing) in the F_1 dimension were recorded for the determination of intermolecular NOEs in a 1:1 [^{15}N]BID-BH3 peptide−[^{13}C]BCL-w complex. Amide heteronuclear ^{15}N{^{1}H} NOEs were measured and used for the identification of high-mobility regions of proteins or peptides (*36*). NMR spectra were processed using NMRPIPE (*37*) and XWIN-NMR (Bruker) and analyzed with XEASY (*38*).

Molecular Modeling. The program High Ambiguity Driven Docking (HADDOCK) (*39*) was used to model the binding of the BID-BH3 peptide to BCL-w. We used Protein Data Bank entry 1MK3 for the structure of the human BCL-w protein (*13*). According to the NMR data, the C-terminal helix of BCL-w was displaced from the hydrophobic cleft by rotation around the HN−C^α chemical bond in Gly-154 and was subsequently considered in the calculations to be unfolded. An atomic coordinate template for the 20-amino acid human BID-BH3 peptide was generated by the Biopolymer module of InsightII (Accelrys) using a standard helical

Table 1: NMR Titration of BCL Proteins by Detergents

	BCL-w with octyl glucoside	BCL-w with DPC	BCL-w−BID-BH3 with DPC	BCL-x_L[a] with DPC	BAX[a] with octyl glucoside
small spectral changes	<5[b]	<0.5	<2	<1	<7
C-terminal helix displacement	10−15	0.5−2	—[c]	—[c]	—[c]
abrupt spectral changes	>20	2−5	2−5	3−5	>20
new protein conformation	—[c]	>5	>5	>5	—[c]

[a] Data for BCL-x_L and BAX proteins are from the literature (*20*, *24*). Critical micelle concentrations are 1−1.5 mM for DPC and 20−25 mM for octyl glucoside. [b] Concentration in millimolar. [c] Not reported or not applicable.

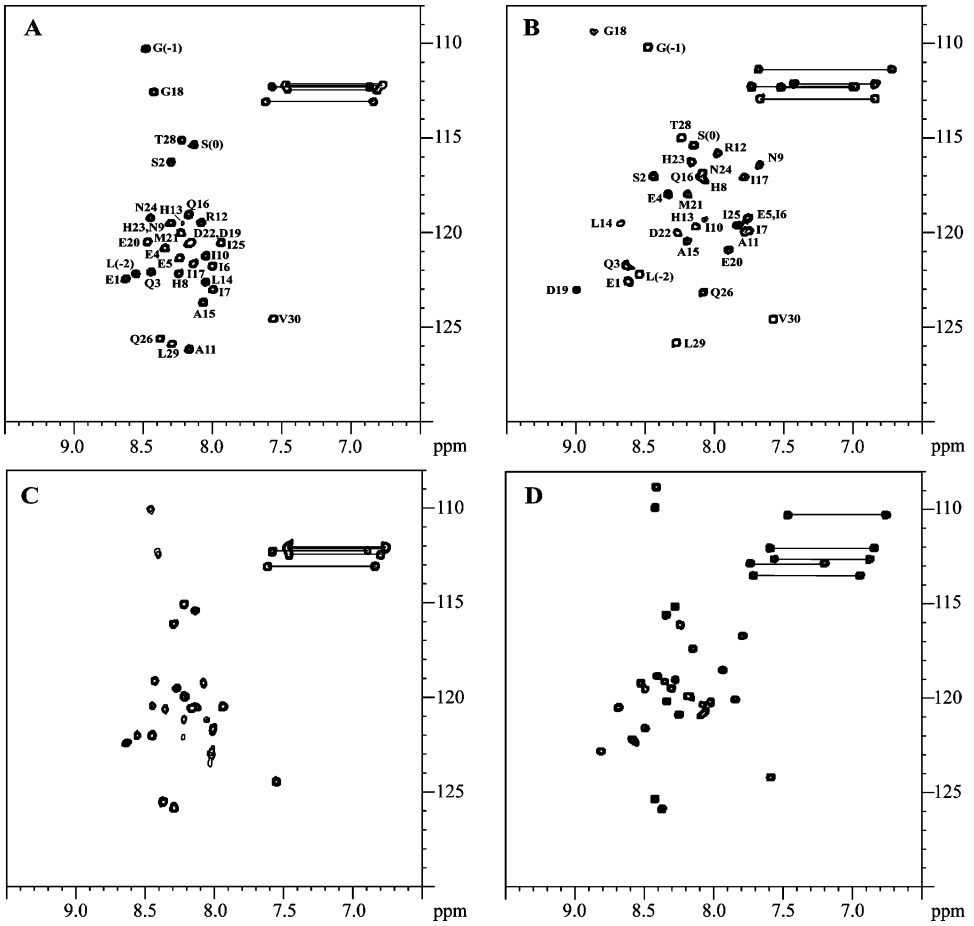

FIGURE 2: Comparison of $^1H-^{15}N$ HSQC spectra of the 30-amino acid mouse BID-BH3 peptide free in solution (A), complexed with unlabeled BCL-w in the absence of detergent (B), and in the presence of 5 mM DPC (C) at 25 °C. The spectrum of the BH3 peptide bound to DPC micelles at 30 mM DPC is shown in panel D. Concentrations of the BID-BH3 peptide and BCL-w were 0.05−0.07 mM. Peptide peak assignments are shown by residue name and number. Horizontal lines indicate the amide signals from Asn and Gln side chains.

conformation, followed by molecular dynamics/mechanics optimization in CNS (*40*). The default HADDOCK parameters were used, except only 200 initial complex structures were generated, and the best 100 solutions in terms of total energies were then refined. Structure figures were generated with MOLMOL (*41*). The pairwise coordinate rmsd comparison between different protein−peptide complex structures was created with DALI (*42*).

RESULTS AND DISCUSSION

Protein Resonance Assignments and NMR Titration with Detergents. In this work, we determined the NMR resonance assignments of 90% of the backbone amides of human wild-type BCL-w in a 1:1 complex with a 20-amino acid human BID-BH3 peptide. Unassigned residues in BCL-w mostly belong to the region around Pro-117, known to be the site of *cis*−*trans*-proline isomerization (*13*). Analysis of NOEs showed that the positions of the BCL-w α-helices in the complex are the same as in the free protein with the notable exception of C-terminal helix α8 which is unfolded in the complex (not shown). The binding of the BID peptide caused the largest chemical shift changes in helices α2−α5 (residues 52−96) and in helices α7 and α8 (residues 150−171; Figure 1, top). Measurement of the heteronuclear $^{15}N\{^1H\}$ NOEs in the complex confirmed the high mobility of the C-terminal region as indicated by the low values for residues 154−171 (hNOEs between 0.1 and 0.6; Figure 1, bottom). For comparison, the values of heteronuclear $^{15}N\{^1H\}$ NOE for the same C-terminal region of BCL-w in the absence of peptide were in range of 0.6−0.7 (*13*). These results suggest that the BH3 peptide binds tightly in the hydrophobic cleft of BCL-w, producing specific conformational rearrangements in BCL-w, including displacement from the cleft and unwinding of C-terminal helix α8.

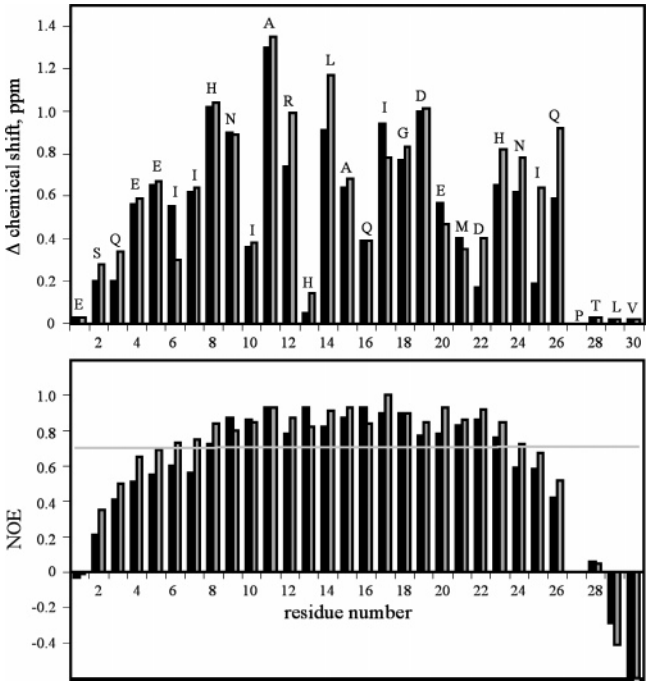

FIGURE 3: Mapping BID-BH3 peptide residues involved in binding. Magnitudes of the amide chemical shift changes (top) and heteronuclear $^{15}N\{^1H\}$ NOEs (bottom) for the mouse BID-BH3 peptide in complex with BCL-w (black bars) and BCL-x_L (gray bars). The horizontal line in the bottom panel corresponds to a heteronuclear NOE of 0.7.

We titrated BCL-w and its complex with the BID peptide with dodecylphosphocholine (DPC) and octyl glucoside and monitored the changes via NMR (Table 1). Similar studies have been reported for BCL-x_L and BAX (*20*, *24*). Our results show that both detergents can displace C-terminal helix α8 of BCL-w from the hydrophobic cleft. However, only DPC led to the formation of a new distinct protein conformation as judged by $^1H-^{15}N$ HSQC spectra in the presence of 5 mM lipid. Further additions of DPC up to 100 mM led to only minor spectral changes (Figure S1 of the Supporting Information). Identical results were observed for BCL-x_L. At 50 mM, the majority of DPC molecules are in micelles. This was confirmed by pulsed-field gradient self-diffusion measurements and ^{31}P NMR spectroscopy. We measured the diffusion coefficients (*D*) of BCL-w at four different DPC concentrations which allowed us to conclude that the complex of BCL-w with 5 mM DPC is considerably larger than what would be expected for the binding of just a few DPC molecules to BCL-w (Figure S2 of the Supporting Information). At the same time, we observed a strong dependence of the size of the BCL/DPC micelles on the DPC concentration up to ~15 mM DPC. These results were mirrored by ^{31}P NMR spectroscopy of micelle formation (Figure S3 of the Supporting Information). The change in the DPC chemical shift at 5 mM DPC corresponds to 40−60% of the total change at 50 mM.

These results suggest that BCL-w is bound to micelles at 5 mM DPC and not to individual lipid molecules. All these changes occurred irrespective of the presence of the BH3 peptide in the solution. Most probably, the structure of this new form of BCL-w is similar to models of BCL-x_L in DPC micelles where hydrophobic helices α5 and α6 are buried in the interior of the micelle (*24*, *25*). At this point, it was unknown whether the BH3 peptide remains folded in the complex with BCL-w when the protein is bound to the membrane.

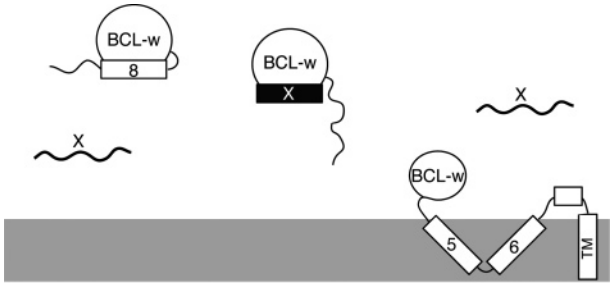

FIGURE 4: Hit-and-run mechanism of the BH3 peptide or a small molecule inhibitor acting on the membrane association of BCL-w. In the first step, the BH3 inhibitor (X) binds in the BCL-w cleft and displaces the C-terminal region of BCL-w which then leads to association with the membrane. In the second step, helices α5 and α6 of BCL-w insert into the membrane as BCL-w adopts its membrane-bound conformation and the inhibitor (X) is released.

BH3 Peptide Resonance Assignments and Regions of Mobility. Thirty-residue ^{15}N-labeled peptides corresponding to the BH3 domain of human and mouse BID were produced biosynthetically and their $^{15}N-^1H$ HSQC spectra fully assigned (Figure 2A). The free peptides were unfolded in solution with negative $^{15}N\{^1H\}$ heteronuclear NOEs for all residues. The binding of the peptides to unlabeled BCL-w and BCL-x_L proteins was investigated. Figures 2B and 3 present the peptide chemical shift changes induced upon binding. The strongest changes were detected for Ala-11, Leu-14, Gly-18, and Asp-19 which are highly conserved in the BH3 regions of all proapoptotic proteins (with the allowance of some Ala/Gly substitutions) (*5*). It is known that the hydrophobic Leu-14 and negatively charged Asp-19 (which hydrogen bonds with the side chain of Arg-139 of BCL-x_L) are highly critical for binding of the BH3 peptide to prosurvival proteins of the BCL-2 family (*17*, *21*−*23*). Despite the obvious changes in chemical shifts, these data alone cannot be used for the precise determination of the BH3 peptide residues which are tightly bound to the BCL-w and BCL-x_L proteins. For example, we detected very small changes for His-13 which is in the middle of the BH3 peptide. To overcome this problem, values of heteronuclear $^{15}N\{^1H\}$ NOEs for BH3 peptide amides were measured (Figure 3). Analysis of these data showed minimal mobility for residues 8−23 of BID-BH3 peptides (NOEs of >0.7). ^{15}N-edited NOESY spectra confirmed that this peptide region is α-helical; medium-range Hα(*i*)−HN(*i* + 3) and other cross-peaks were detected and used as NOE restraints in structure calculations. The BCL-x_L−BAD peptide and BCL-x_L−BAK peptide structures (*21*, *22*) exhibit similar binding regions and helicities for the BH3 peptides, although the helical portion is extended at the C-terminus in the BCL-x_L−BIM peptide complex (*23*).

Characterization of the Complex in Micelles. The mouse and human ^{15}N-labeled BID-BH3 peptides and their complexes with unlabeled BCL-w were titrated with DPC. Both BID-BH3 peptides in the absence of BCL-w protein exhibited binding to micelles at DPC concentrations above 10−15 mM but not at 5 mM (Figure 2D). The structures of BID-BH3 peptide−micelle complexes are under further investigation; these probably represent surface-bound α-helices as proposed for tBID (*26*).

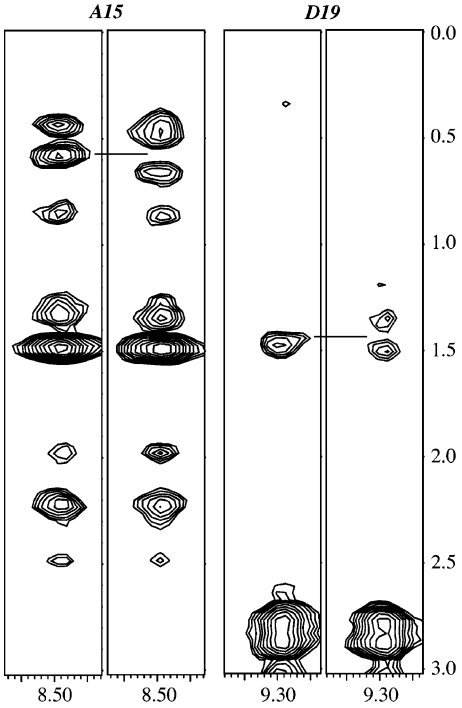

FIGURE 5: Determination of protein−peptide intermolecular NOEs. Two-dimensional $^{1}H-^{1}H$ planes taken from a pair of three-dimensional ^{15}N-edited NOESY spectra with (left) and without (right) ^{13}C decoupling in the F_1 dimension. Strips are shown for peptide signals, Ala-15 and Asp-19, in a complex of ^{15}N-labeled human BID-BH3 and ^{13}C-labeled BCL-w. Intermolecular NOEs are doublets in the coupled spectrum, whereas intramolecular NOEs are singlets in both spectra. Intermolecular NOEs between HN(Ala-15) and CH_3(Leu-86) and between HN(Asp-19) and CH_3(Ala-98) are indicated by horizontal lines.

In contrast to the simple titration behavior observed with free peptides or isolated BCL proteins, addition of DPC to a complex of the ^{15}N-labeled BID-BH3 peptide bound to BCL-w led to a biphasic behavior. Addition of intermediate DPC (5−6 mM) concentrations led to changes in the BID-BH3 peptide spectrum that coincided with the spectrum of the free form of the peptide (Figures 2A and 2C). These peptide signals also exhibited negative heteronuclear $^{15}N-\{^{1}H\}$ NOEs (data not shown). The amide HSQC peaks for Ala-11, Gln-16, and Ile(Val)-17 were very weak, possibly due to exchange processes. In the same sample, the formation of a micelle-bound conformation of BCL-w was observed as detected by the characteristic $H_\epsilon 1$ side chain Trp signals in one-dimensional NMR spectra (see also Figure S1 of the Supporting Information). These spectra reveal that the BH3 peptide is released in solution after addition of 5−6 mM DPC.

In the second phase, further increasing the DPC concentration (up to 50 mM) led to BH3 peptide HSQC spectra which were typical for micelle-bound BID-BH3 peptides in the absence of the BCL-w protein (Figure 2D). Identical results were obtained for the BCL-x_L−BID-BH3 peptide titrations with DPC. We also performed octyl glucoside titrations with the peptide complexes, but these were not informative because BCL-w did not adopt a new conformation that could be identified by NMR and octyl glucoside did not disrupt the BCL-w−BID-BH3 peptide complex in the range of concentrations that was studied (up to 100 mM).

These results demonstrate that when BCL-w or BCL-x_L forms a new stable conformation in DPC micelles, the BID-BH3 peptide is released into solution as an unfolded peptide. At higher detergent concentrations, the released BID-BH3 peptide can also bind to the micelles. The implications for the behavior of tBID or the full-length BIM protein under similar conditions need to be investigated because the intact proteins contain multiple hydrophobic segments and most probably remain bound to the membrane (separately or as part of the BCL-w complex). However, our result is relevant for our understanding of the catalytic action of small molecules and BH3 inhibitors on prosurvival proteins of the BCL-2 family (*43*−*46*). Previous studies (*34*) have shown that membrane binding of BCL-w is stimulated by a BIM peptide but the peptide localization was not addressed. Our results suggest a "hit-and-run" mechanism for BH3 peptide and small molecule inhibitors (Figure 4). In light of recent results for BCL-x_L, BCL-2, and BAX proteins, which confirmed directly the insertion of transmembrane region and helices α5 and α6 into the membrane (*29*, *47*, *48*), the general scheme could easily be extended to suggest that all BCL proteins lose their BH3-binding site upon the conformational change associated with membrane binding.

Structure of the BCL-w−BH3 Peptide Complex. Our studies showed that the 16 central residues of BID-BH3 peptides suffice for complex formation. To gain further insight, we calculated the structure of BCL-w with the 20-amino acid human BID-BH3 peptide. On the basis of our finding that the BID-BH3 peptide displaces C-terminal helix α8 from the BCL-w hydrophobic cleft and forms its own

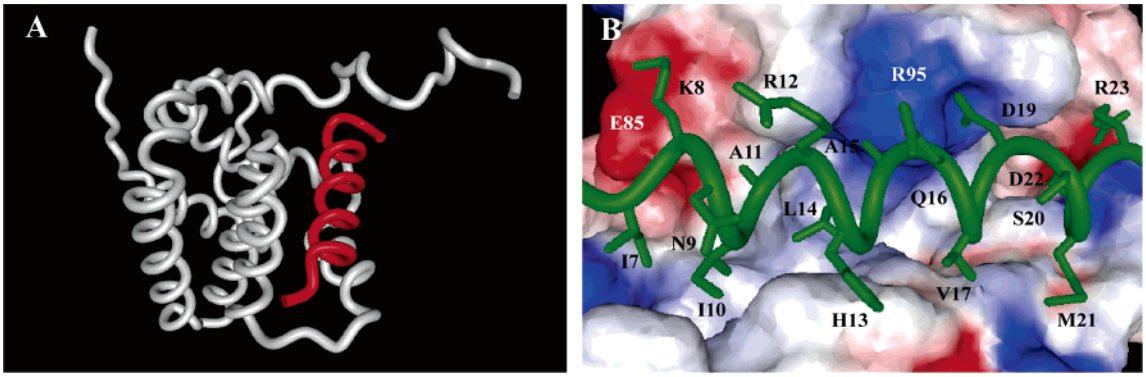

FIGURE 6: NMR-derived models of the BCL-w−BID-BH3 peptide complex using HADDOCK. (A) Backbone view of the best structure. The C-terminal region of BCL-w in complex with the BID-BH3 peptide is unfolded. (B) Surface presentation of the binding cleft of BCL-w bound to the BID peptide.The surface of BCL-w is color-coded, with red indicating negative electrostatic potential and blue indicating positive potential. Residues of the BID-BH3 peptide are labeled in black and those of the BCL-w protein in white.

Table 2: Experimental Restraints and Structural Statistics

docking restraints	
no. of ambiguous interaction restraints (AIRs)	16
no. of medium-range and intermolecular NOEs	17
no. of hydrogen bonds in BH3 peptide	12
no. of ϕ backbone angles in BH3 peptide	16
final energy (kcal/mol)	
E_{total}	-620 ± 50
E_{vdw}	-90 ± 23
E_{elec}	-538 ± 49
E_{NOE}	0.07 ± 0.06
E_{cdih}	0.33 ± 0.29
rmsd for experimental restraints	
distances (Å)	0.043 ± 0.025
dihedral angles (deg)	0.33 ± 0.17
coordinate rmsd from average structure (Å)[a]	
backbone atoms (N, C^α, C′)	0.76 ± 0.09
all heavy atoms	0.94 ± 0.09
Ramachandran analysis (%)	
residues in most favored regions	85.6 ± 1.8
residues in additional allowed regions	12.8 ± 2.2
residues in generously allowed regions	1.8 ± 1.2

[a] For residues 10−24 and 42−153 of BCL-w and 16 core residues in the BH3 peptide.

α-helix of a similar size in the same cleft, we decided to limit our modeling to a simple docking protocol. HSQC chemical shift changes for both BCL-w and the BH3 peptide were used as HADDOCK distance constraints along with additional intermolecular NOEs from ^{13}C- and ^{15}N-edited NOESY experiments (Figure 5). This provided two medium to strong NOE contacts between HN(Ala-11) and Me(Val-82) and between HN(Ala-15) and Me(Leu-86) and two weak NOEs between HN(Gly-18) and Me(Ala-98) and between HN(Asp-19) and Me(Ala-98), which gave the proper orientation for the BH3 peptide in the BCL-w cleft.

The general structure of the BCL-w−BID-BH3 peptide complex is presented in Figure 6A, and the structural statistics for the 10 best structures are shown in Table 2. The BH3 peptide occupies the hydrophobic cleft of BCL-w and forces the unfolding and high mobility of the C-terminal BCL-w α-helix. The pairwise C^α atomic coordinate rmsds between the BCL-w−BID peptide complex structure (for inflexible residues 10−24 and 42−153 in BCL-w and the 16 core residues in the BID-BH3 peptide) and BCL-x_L−BAK, −BAD, or −BIM peptide complexes (*21*−*23*) are 2.9−3.3 Å (DALI *Z* factors = 8.9−11.1). Detailed structural analysis confirms the hydrogen bond between side chains in Asp-19 of the BID-BH3 peptide and Arg-95 in helix α5 of BCL-w (Figure 6B). The side chain of another important Leu-14 residue is oriented toward the surface of the BCL-w hydrophobic cleft. In addition, the imidazole group of His-13 is directed into solution, which could partially explain the small shift of the amide $^1H-^{15}N$ signal for this residue during binding of the BH3 peptide to BCL-w (Figure 3).

In conclusion, our results suggest that the BCL-w−BID-BH3 peptide complex has a structure similar to known BCL-x_L−BH3 peptide structures. Studies of the interactions of a BCL-w−BH3 peptide complex with micelles reveal that release of the BH3 peptide occurs when BCL-w binds to the micelle. This suggests that the BH3 peptide binding site is lost in the lipid-bound conformation of BCL-w. These results are relevant for understanding the apoptotic action of small molecule inhibitors of prosurvival BCL-2 family members and models of their action.

ACKNOWLEDGMENT

We thank Gordon C. Shore for comments and interest in the manuscript.

SUPPORTING INFORMATION AVAILABLE

Comparison of $^1H-^{15}N$ HSQC spectra of BCL-w in the absence and presence of DPC, pulsed-field gradient NMR self-diffusion measurements of BCL-w and BCL-x_L in DPC micelles, and ^{31}P chemical shifts of DPC in the absence and presence of 0.1 mM BCL-w as a function of DPC concentration. This material is available free of charge via the Internet at http://pubs.acs.org.

REFERENCES

1. Danial, N. N., and Korsmeyer, S. J. (2004) Cell death: Critical control points, *Cell 116*, 205−219.
2. Cory, S., Huang, D. C. S., and Adams, J. M. (2003) The Bcl-2 family: Roles in cell survival and oncogenesis, *Oncogene 22*, 8590−8607.
3. Strasser, A. (2005) The role of BH3-only proteins in the immune system, *Nat. Rev. Immunol. 5*, 189−200.
4. Kaufmann, T., Schinzel, A., and Borner, C. (2004) Bcl-w(edding) with mithochondria, *Trends Cell Biol. 14*, 8−12.
5. Chen, L., Willis, A., Wei, A., Smith, B. J., Fletcher, J. I., Hinds, M. G., Colman, P. M., Day, C. L., Adams, J. M., and Huang, D. C. S. (2005) Differential targeting of prosurvival Bcl-2 proteins by their BH3-only ligands allows complementary apoptotic function, *Mol. Cell 17*, 393−403.
6. Kuwana, T., Bouchier-Hayes, L., Chipuk, J. E., Bonzon, C., Sullivan, B. A., Green, D. R., and Newmeyer, D. D. (2005) BH3 domains of BH3-only proteins differentially regulate Bax-mediated mitochondrial membrane permeabilization both directly and indirectly, *Mol. Cell 17*, 525−535.
7. Pagliari, L. J., Kuwana, T., Bonzon, C., Newmeyer, D. D., Tu, S., Beere, H. M., and Green, D. R. (2005) The multidomain proapoptotic molecules Bax and Bak are directly activated by heat, *Proc. Natl. Acad. Sci. U.S.A. 102*, 17975−17980.
8. Chipuk, J. E., Kuwana, T., Bouchier-Hayes, L., Droin, N. M., Newmeyer, D. D., Schuler, M., and Green, D. R. (2004) Direct activation of Bax by p53 mediates mitochondrial membrane permeabilization and apoptosis, *Science 303*, 1010−1014.
9. Leu, J. I., Dumont, P., Hafey, M., Murthy, M. E., and George, D. L. (2004) Mitochondrial p53 activates Bak and causes disruption of Bak-Mcl1 complexes, *Nat. Cell Biol. 6*, 443−450.
10. Petros, A. M., Olejniczak, E. T., and Fesik, S. W. (2004) Structural biology of the Bcl-2 family of proteins, *Biochim. Biophys. Acta 1644*, 83−94.
11. Muchmore, S. W., Sattler, M., Liang, H., Meadows, R. P., Harlan, J. E., Yoon, H. S., Nettesheim, D., Chang, B. S., Thompson, C. B., Wong, S. L., Ng, S. C., and Fesik, S. W. (1996) X-ray and NMR structure of human Bcl-xL, an inhibitor of programmed cell death, *Nature 381*, 335−341.
12. Aritomi, M., Kunishima, N., Inohara, N., Ishibashi, Y., Ohta, S., and Morikawa, K. (1997) Crystal structure of rat Bcl-xL. Implications for the function of the Bcl-2 protein family, *J. Biol. Chem. 272*, 27886−27892.
13. Denisov, A. Y., Madiraju, M. S. R., Chen, G., Khadir, A., Beauparlant, P., Attardo, G., Shore, G. C., and Gehring, K. (2003) Solution structure of human BCL-w: Modulation of ligand binding by the C-terminal helix, *J. Biol. Chem. 278*, 21124−21128.
14. Hinds, M. G., Lackmann, M., Skea, G. L., Harrison, P. J., Huang, D. C. S., and Day, C. L. (2003) The structure of Bcl-w reveal a role for the C-terminal residues in modulating biological activity, *EMBO J. 22*, 1497−1507.
15. Petros, A. M., Medek, A., Nettesheim, D. G., Kim, D. H., Yoon, H. S., Swift, K., Matayoshi, E. D., Oltersdorf, T., and Fesik, S. W. (2001) Solution structure of the antiapoptotic protein Bcl-2, *Proc. Natl. Acad. Sci. U.S.A. 98*, 3012−3017.
16. Huang, Q., Petros, A. M., Virgin, H. W., Fesik, S. W., and Olejniczak, E. T. (2002) Solution structure of a Bcl-2 homolog from Kaposi sarcoma virus, *Proc. Natl. Acad. Sci. U.S.A. 99*, 3428−3433.

17. Day, C. L., Chen, L., Richardson, S. J., Harrison, P. J., Huang, D. C. S., and Hinds, M. G. (2005) Solution structure of prosurvival Mcl-1 and characterization of its binding by proapoptotic BH3-only ligands, *J. Biol. Chem. 280*, 4738−4744.
18. Chou, J. J., Li, H., Salvesen, G. S., Yuan, J., and Wagner, G. (1999) Solution structure of BID, an intracellular amplifier of apoptotic signaling, *Cell 96*, 615−624.
19. McDonnell, J. M., Fushman, D., Milliman, C. L., Korsmeyer, S. J., and Cowburn, D. (1999) Solution structure of the proapoptotic molecule BID: A structural basis for apoptotic agonists and antagonists, *Cell 96*, 625−634.
20. Suzuki, M., Youle, R. J., and Tjandra, N. (2000) Structure of Bax: Coregulation of dimer formation and intracellular localization, *Cell 103*, 645−654.
21. Sattler, M., Liang, H., Nettesheim, D., Meadows, R. P., Harlan, J. E., Eberstadt, M., Yoon, H. S., Shuker, S. B., Chang, B. S., Minn, A. J., Thompson, C. B., and Fesik, S. W. (1997) Structure of Bcl-xL-Bak peptide complex: Recognition between regulators of apoptosis, *Science 275*, 983−986.
22. Petros, A. M., Nettesheim, D. G., Wang, Y., Olejniczak, E. T., Meadows, R. P., Mack, J., Swift, K., Matayoshi, E. D., Zhang, H., Thompson, C. B., and Fesik, S. W. (2000) Rationale for Bcl-xL/Bad peptide complex formation from structure, mutagenesis, and biophysical studies, *Protein Sci. 9*, 2528−2534.
23. Liu, X., Dai, S., Zhu, Y., Marrack, P., and Kapper, J. W. (2003) The structure of a Bcl-xL/Bim fragment complex: Implications for Bim function, *Immunity 19*, 341−352.
24. Losonczi, J. A., Olejniczak, E. T., Betz, S. F., Harlan, J. E., Mack, J., and Fesik, S. W. (2000) NMR studies of the anti-apoptotic protein Bcl-xL in micelles, *Biochemistry 39*, 11024−11033.
25. Franzin, C. M., Choi, J., Zhai, D., Reed, J. C., and Marassi, F. M. (2004) Structural studies of apoptosis and ion transport regulatory proteins in membranes, *Magn. Reson. Chem. 42*, 172−179.
26. Gong, X. M., Choi, J., Franzin, C. M., Zhai, D., Reed, J. C., and Marassi, F. M. (2004) Conformation of membrane-associated proapoptotic tBid, *J. Biol. Chem. 279*, 28954−28960.
27. Liang, H., and Fesik, S. W. (1997) Three-dimensional structures of proteins involved in programmed cell death, *J. Mol. Biol. 274*, 291−302.
28. Oh, K. J., Barbuto, S., Meyer, N., Kim, R. S., Collier, J., and Korsmeyer, S. J. (2005) Conformational changes in BID, a pro-apoptotic BCL-2 family member, upon membrane binding, *J. Biol. Chem. 280*, 753−767.
29. Kim, P. K., Annis, M. G., Dlugosz, P. J., Leber, B., and Andrews, D. W. (2004) During apoptosis Bcl-2 changes membrane topology at both endoplasmic reticulum and mitochondria, *Mol. Cell 14*, 523−529.
30. Terrones, O., Antonsson, B., Yamaguchi, H., Wang, H. G., Liu, J., Lee, R. M., Herrmann, A., and Basanez, G. (2004) Lipid pore formation by the concerted action of proapoptotic BAX and tBID, *J. Biol. Chem. 279*, 30081−30091.
31. Wilson, J. W., Nostro, M. C., Balzi, M., Faraoni, P., Cianchi, F., Becciolini, A., and Potten, C. S. (2000) Bcl-w expression in colorectal adenocarcinoma, *Br. J. Cancer 82*, 178−185.
32. Print, C. G., Loveland, K. L., Gibson, L., Meehan, T., Stylianou, A., Wreford, N., de Kretser, D., Metcalf, D., Kontgen, F., Adams, J. M., and Cory, S. (1998) Apoptosis regulator Bcl-w is essential for spermatogenesis but appears otherwise redundant, *Proc. Natl. Acad. Sci. U.S.A. 95*, 12424−12431.
33. Meehan, T., Loveland, K. L., de Kretser, D., Cory, S., and Print, C. G. (2001) Developmental regulation of the bcl-2 family during spermatogenesis: Insights into the sterility of bcl-w$^{-/-}$ male mice, *Cell Death Differ. 8*, 225−233.
34. Wilson-Annan, J., O'Reilly, L. A., Crawford, S. A., Hausmann, G., Beaumont, J. G., Parma, L. P., Chen, L., Lackmann, M., Lithgow, T., Hinds, M. G., Day, C. L., Adams, J. M., and Huang, D. C. S. (2003) Proapoptotic BH3-only proteins trigger membrane integration of prosurvival Bcl-w and neutralize its activity, *J. Cell Biol. 162*, 877−887.
35. Cavanagh, J., Fairbrother, W. J., Palmer, A. G., and Skelton, N. J. (1996) *Protein NMR Spectroscopy: Principles and Practice*, Academic Press, San Diego.
36. Peng, J. W., and Wagner, G. (1994) Investigation of protein motions via relaxation measurements, *Methods Enzymol. 239*, 563−596.
37. Delaglio, F., Grzesiek, S., Vuister, G. W., Zhu, G., Pfeifer, J., and Bax, A. (1995) NMRpipe: A multidimensional spectral processing system based on UNIX pipes, *J. Biomol. NMR 6*, 277−293.
38. Bartels, C., Xia, T. H., Billeter, M., Guntert, P., and Wüthrich, K. (1995) The program XEASY for computer-supported NMR spectral analysis of biological macromolecules, *J. Biomol. NMR 5*, 1−10.
39. Domingues, C., Boelens, R., and Bonvin, A. M. J. J. (2003) HADDOCK: A protein−protein docking approach based on biochemical or biophysical information, *J. Am. Chem. Soc. 125*, 1731−1737.
40. Brünger, A. T., Adams, P. D., Clore, G. M., DeLano, W. L., Gros, P., Grosse-Kuntsleve, R. W., Jiang, J. S., Kuszewski, J., Nilges, M., Pannu, N. S., Read, R. J., Rice, L. M., Simonson, T., and Warren, G. L. (1998) Crystallography and NMR system: A new software suite for macromolecular structure determination, *Acta Crystallogr. D54*, 905−921.
41. Koradi, R., Billeter, M., and Wüthrich, K. (1996) MOLMOL: A progam for display and analysis of macromolecular structures, *J. Mol. Graphics 14*, 51−55.
42. Holm, L., and Sander, C. (1993) Protein structure comparison by alignment of distance matrices, *J. Mol. Biol. 233*, 123−138.
43. Lugovskoy, A. A., Degterev, A. I., Fahmy, A. F., Zhou, P., Gross, J. D., Yuan, J., and Wagner, G. (2002) A novel approach for characterizing protein ligand complexes: Molecular basis for specificity of small-molecule Bcl-2 inhibitors, *J. Am. Chem. Soc. 124*, 1234−1240.
44. Kitada, S., Leone, M., Sareth, S., Zhai, D., Reed, J. C., and Pellecchia, M. (2003) Discovery, characterization, and structure−activity relationships studies of proapoptotic polyphenol targeting B-cell lymphocyte/leukemia-2 proteins, *J. Med. Chem. 46*, 4259−4264.
45. Yin, H., Lee, G. I., Sedey, K. A., Rodriguez, J. M., Wang, H. G., Sebti, S. M., and Hamilton, A. D. (2005) Terephthalamide derivatives as mimetics of helical peptides: Disruption of the Bcl-x(L)/Bak interaction, *J. Am. Chem. Soc. 127*, 5463−5468.
46. Oltersdorf, T., Elmore, S. W., Shoemaker, A. R., Armstrong, R. C., Augeri, D. J., Belli, B. A., Bruncko, M., Deckwerth, T. L., Dinges, J., Hajduk, P. J., Joseph, M. K., Kitada, S., Korsmeyer, S. J., Kunzer, A. R., Letai, A., Li, C., Mitten, M. J., Nettesheim, D. G., Ng, S., Nimmer, P. M., O'Connor, J. M., Oleksijew, A., Petros, A. M., Reed, J. C., Shen, W., Tahir, S. K., Thompson, C. B., Tomaselli, K. J., Wang, B., Wendt, M. D., Zhang, H., Fesik, S. W., and Rosenberg, S. H. (2005) An inhibitor of Bcl-2 family proteins induces regression of solid tumors, *Nature 435*, 677−681.
47. Annis, M. G., Soucie, E. L., Dlugosz, P. J., Cruz-Aguado, A., Penn, L. Z., Leber, B., and Andrews, D. W. (2005) Bax forms multispanning monomers that oligomerize to permeabilize membranes during apoptosis, *EMBO J. 24*, 2096−2103.
48. Jeong, S. Y., Gaume, B., Lee, Y. J., Hsu, Y. T., Ryu, S. W., Yoon, S. H., and Youle, R. J. (2004) Bcl-xL sequesters its C-terminal membrane anchor in soluble, cytosolic homodimers, *EMBO J. 23*, 2146−2155.

BI052332S